

# Influence of low-cycle fatigue and corrosion phenomena on the structural behaviour of steel reinforcing bars



**S. Caprili, W. Salvatore**

*Department of Civil Engineering, University of Pisa, Italy*

**F. Braga, R. Gigliotti**

*Department of Structural and geotechnical engineering, University of Rome La Sapienza, Italy*

**A. Braconi**

*RIVA FIRE SpA, Politiche di Ricerca – Prodotti Lunghi, Milano, Italy*

## SUMMARY:

Modern design standards for r.c. buildings allow the achievement of ductile structures, able to globally dissipate seismic energy through the development of plastic deformations in the dissipative regions. The hysteretic capacity of r.c. structures is related to the ability of reinforcing steel rebars of sustaining many cycles of high plastic deformations (Low-Cycle Fatigue); this condition shall consequently be widely investigated taking into account also the effects of corrosion phenomena, often leading to the decrease of the mechanical characteristics of rebars (strength and ductility). In the present paper, elaborated inside the European research project Rusteel, a detailed experimental investigation of the mechanical capacity of rebars under the combined effects of LCF and corrosion is carried out, as well as the deep analysis of the effective seismic demand on steel reinforcements, evaluated through the execution of non linear incremental dynamic analysis on opportune r.c. case studies designed according to actual design standards.

*Keywords: Low-Cycle Fatigue, corrosion phenomena, ductility, IDA*

## 1. INTRODUCTION AND METHODOLOGY

Reinforced concrete buildings in seismic areas, actually designed according to Eurocode 8 (UNI EN 1998-1-1:2005), follow the hierarchy principles of the *capacity design* approach, as regards both strength of structural elements (i.e. weak beam - strong column) and collapse modalities (i.e. flexural global mechanisms instead of brittle local ones). The global dissipation of the seismic energy stored in the building during an earthquake is strictly influenced by the ability of structural elements to sustain high rotations in correspondence of the dissipative zones, located at the ends of the element; moreover, the rotational capacity of structural members depends on the ductility capacity of steel reinforcing bars located in the end sections, expressed in terms of elongation to maximum load ( $A_{gt}$ ). The ability of the structure to develop and sustain high plastic deformations is mainly related to two aspects, that are the structural details of the dissipative zones and the mechanical characteristics of the longitudinal and transversal reinforcements used.

Eurocode 8 allows the use of steel rebars belonging to three different ductility classes, called “A”, “B” and “C” in relation to the level of available  $A_{gt}$ , respectively equal to 2.5%, 5.0% or 7.5% and to the value of hardening ratio, respectively  $\geq 1.05$ ,  $\geq 1.08$  and between 1.15 and 1.35, as well as presented in Annex C of Eurocode 2 (UNI EN 1992-1-1:2005). For buildings realized in high ductility class (HDC), the only use of class C is allowed for longitudinal steel reinforcements, while for buildings in low ductility class (LDC) both classes B and C are authorized. Italian standards for constructions (D.M. 14/01/2008) in addition to what herein presented, allows, only for stirrups, a low requirement of ductility (class A). The limits herein presented are related to the monotonic behaviour of reinforcements, while no specific indications are given as regards their seismic requirements (Low-Cycle Fatigue condition – LCF).

The investigation of the LCF behaviour of steel reinforcing bars in dissipative zones of structural elements is obviously necessary for the understanding of the global dynamic behaviour of r.c. buildings. Actually, at European level, no specific rules for the seismic qualification of steel rebars are

provided: only Spain and Portugal (UNE 36065 EX, LNEC E455-2008 and LNEC E460-2008) introduce indications for the execution of LCF tests, in which, nevertheless, the levels of imposed deformation, the test frequency, the free length of the specimen and the number of cycles to execute are not defined in relation to scientific considerations or analysis.

Actually, the ductility requirements imposed by Eurocode 8 and 2 are generally satisfied by the use of TempCore steel rebars; TempCore process, through the two mechanical phases of quenching and heating, is able to provide high levels of yielding strength and ductility with moderate production costs. Micro Alloyed steel rebars, through the addition of alloyed elements (such as Vanadium, Nickel or others) also allow the achievement of high mechanical characteristics, but the costs associated to their production process are higher respect to TempCore, so that their diffusion is strongly limited.

Despite their large use in r.c. structures, recent works in the current literature (Apostolopoulos and Papadopoulos 2007, Apostolopoulos and Papadakis 2008) evidenced the decrease of the mechanical properties of TempCore rebars under aggressive environmental conditions (i.e. chloride exposition), both in terms of strength (yielding and tensile stress,  $R_e$  and  $R_m$ ) and ductility ( $A_{gt}$ ).

Even if the actual prescriptions for the sizing of the concrete cover (UNI EN 1992-1:2005) should prevent spalling protecting steel reinforcements, the knowledge of the mechanical behaviour of rebars after corrosion is necessary both for the monotonic and the cyclic loading conditions.

On the base of what herein presented and taking into account the necessity of European standards' harmonization imposed by Mandate M115 inside the revision of EN10080, a detailed campaign of experimental tensile and LCF tests on uncorroded and corroded rebars was developed in the framework of a European research project funded by the Research Fund for Coal and Steel, called *Rusteel (Effects of Corrosion on Low-Cycle Fatigue (Seismic) Behaviour of High Strength Steel Reinforcing Bar*, 2012). The *Rusteel* project is organized into two main different branches: the first is related to the investigation of the effective *ductility capacity* of steel reinforcements, opportunely determined with the execution of experimental mechanical tests (tensile and LCF) on uncorroded and corroded bars; the second deals with the evaluation of the real *ductility demand* imposed by earthquakes to steel reinforcements in structural elements, determined through the execution of non linear Incremental Dynamic Analyses (IDA) on r.c. case studies. The comparison between experimental and numerical results (i.e. between demand and capacity) will allow the individuation of the link between Corrosion Damage Indicators (CDI), related to the effects of corrosion on rebars (i.e. mass loss), and Performance Indicators (PI), related to the mechanical properties of the rebars (i.e. diameter, steel grade, ductility and production process), leading to the definition, for example, of the exposure time required for generating a specific level of detrimental effects on steel reinforcements.

In the present paper, the results obtained by the experimental test campaign on uncorroded and corroded rebars and the ductility demand given by preliminary numerical analyses on a residential r.c. case study are presented.

## **2. DUCTILITY CAPACITY OF STEEL REBARS**

### **2.1. Tensile and Low-Cycle Fatigue mechanical characterization**

A representative set of steel rebars, including different mechanical production processes - TempCore (TEMP), Micro-Alloyed (MA), Stretched (STR) and Cold-Worked (CW), different yielding strength (400, 450 and 500 MPa), ductility classes (A, B and C) and diameters (between 8 and 25 mm) - was selected inside *Rusteel* project for the complete mechanical characterization of the actual European production of steel reinforcing bars. The experimental test campaign includes both tensile and LCF tests, executed following the protocol elaborated inside the research project. In Table 2. the selected steel grades and diameters are presented; the asterisk indicates the rebars subjected to LCF tests.

The significant parameter affecting the execution of LCF tests, i.e. the level of imposed deformation ( $\epsilon$ ) and the frequency of load application (i.e. strain rate), the number of cycles ( $N_f$ ) and the free length of the specimen ( $L_0$ ) were defined according to the indications given by actual literature and standards. Nowadays, only Spain and Portugal provide indications for the seismic qualification of steel rebars (UNE 36065 EX, LNEC E455/460-2008), prescribing the execution of LCF tests in which three or ten cycles, respectively, shall be executed with a level of imposed deformation equal to  $\pm 1.0\%$ ,  $\pm 2.5\%$  or  $\pm 4.0\%$  in relation to the diameter ( $\phi \leq 16$  mm,  $16 < \phi \leq 25$  mm and  $\phi \geq 25$  mm, UNE 36065 EX) or

simply equal to  $\pm 2.5\%$  (Portuguese standard); the free length varies with the size of rebars (Spain) or is fixed equal to 10 diameters (Portugal). A testing frequency equal to 3.0 Hz is prescribed by LNEC E455/E460-2008.

At the same time, different works in the current literature (Mander et al, 1994, Rodriguez et al. 1999, Hawileh et al. 2010) evidenced the possibility of executing LCF tests with a reduced frequency with respect to what actually presented by standards, equal to 0.05 Hz or also lower (i.e. 0.005 Hz); as regards to the free length to use, experimental tests executed on specimens with  $L_0$  between 6 and 10 times the bar diameter showed, in general, buckling phenomena of rebars for  $L_0$  higher than  $6\phi$ .

On the base of the presented data, a specific protocol for LCF tests was elaborated, including all the significative factors herein listed. According to actual European and Italian standards (UNI EN 1998-1:2005, D.M. 14/01/2008) the maximum stirrups' spacing cannot exceed  $6\phi$  or  $8\phi$  in relation to the ductility class adopted in the desing ( $6\phi$  for HDC,  $8\phi$  for LDC).

For the execution of *Rusteel* low-cycle fatigue test's campaign, the above two different free lengths were selected, representing the situation of both HDC and LDC buildings; two different levels of imposed deformation were adopted, respectively equal to  $\pm 2.5\%$  and  $\pm 4.0\%$ , the maximum number of cycles to execute was fixed at 20 and the frequency used equal to 2.0 Hz (reduced to 0.05 Hz in relation to mechanical requirements of instrumentation for diameters higher than 16 mm). LCF tests were executed using a machine with 250 kN capacity in deformation control, imposing  $\Delta l = \pm \varepsilon \cdot L_0$  on all the bars provided by asterisk presented in Table 2.1. The results of preliminary tests showed buckling phenomena of steel reinforcements after one-two cycles in compression, both for small and large diameters and for a free length of 6 or 8 diameters; for  $L_0=6\phi$  and imposed deformation equal to  $\pm 2.5\%$  rebars were, in general, able to support 20 cycles tension/compression without failure, with buckling phenomena after the first one or two cycles in compression. 20 cycles were also obtained from rebars of small diameter for the same level of deformation in LDC ( $L_0=8\phi$ ). The number of cycles completed decreases with the increase of the deformation level required and of the diameter: for bars of 20 mm diameter and deformation of  $\pm 4.0\%$  the maximum number of complete cycles is equal to 7 ( $L_0=8\phi$ ); for bars of 8.0 mm diameter and a free length of  $6\phi$ , the specimens are able to complete at least 12 cycles. Figure 1 presents the load - deformation diagrams obtained from LCF tests on bars B500B, diameter 16 mm, TempCore for HDC and LDC and deformation equal to  $\pm 2.5\%$  and  $\pm 4.0\%$ .

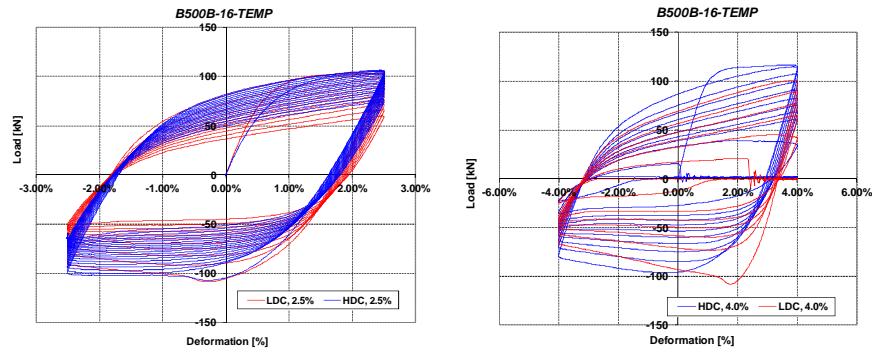


**Figure 2.1.** LCF tests for deformations  $\pm 2.5\%$  and  $\pm 4.0\%$  on bars B500B, 16 mm TempCore,  $L_0=6\phi$  and  $L_0=8\phi$ .

**Table 2.1.** Selected set of rebars for the mechanical characterization.

Steel Grade	Diameter	Steel Process	Ribs	Furniture	More information
B500A	8*, 12*	CW	ribbed	Prod.1	
B500A	8*	CW	indented	Prod.2	
B500B	8*, 16*, 20*, 25	TEMP	ribbed	Prod.1	Same cast for all diameters
	16*			Prod.2	From 3 different plants
B500B	8*, 12	STR	ribbed	Prod.2	German plants
B400C	8*, 16*, 20*, 25	TEMP	ribbed	Prod.2	Spanish plants
B400C	16*, 20*, 25	MA	ribbed	Prod.1	Same cast for all diameters
B450C	16*, 20*, 25	TEMP	ribbed	Prod.1	Same cast for all diameters
	16			Prod.2	From 3 different plants
B450C	8*, 12*	STR	ribbed	Prod. 1+2	

## 2.2. Corrosion phenomena on steel rebars: influence on the mechanical properties

Recent studies in the current literature (Apostolopoulos and Papadopoulos 2007, Apostolopoulos 2007, Apostolopoulos and Papadakis 2008) showed the negative effects of corrosion phenomena on the mechanical behaviour of steel reinforcements under monotonic and cyclic loading conditions.

According to actual design standards for constructions (UNI EN 1992-1-1:2005), corrosion phenomena on steel reinforcing bars can be simply avoided introducing an opportune concrete cover, whose dimensions are related to different exposure classes (XC, corrosion due to carbonation, XD and XS corrosion due to chlorides and XF, corrosion due to de-icing cycles): bars embedded in the concrete pore solution are provided of a protective passive layer that is stable for a pH level of about 12.8. The entry of CO<sub>2</sub> in the concrete (especially in old structures) or the presence of chlorides (especially for those buildings located in proximity of the seaside) can lower the pH of the pore solution to values below 11, for which the corrosion phenomena begin to spread, due to the cracking of the protective passive layer, and deterioration processes of steel rebars can run on.

The main consequences of corrosion phenomena on the mechanical behaviour of steel reinforcing bars can be summarized in to three aspects: the first consists in the mass loss, due to the generation of rust in correspondence of the exposed length, leading to the reduction of effective cross section of the rebar and resulting in a decrease of the bearing capacity of the reinforcement; the second is the spalling of the concrete cover, that allows buckling phenomena of steel rebars in compression and the third, widely investigated and of particular importance for seismic applications (Apostolopoulos and Papadakis 2008, Apostolopoulos and Michalopoulos 2006), is the reduction of the ductility of the bar, expressed in terms of elongation to maximum load ( $A_{gt}$ , or to total elongation  $A$  or  $\epsilon_u$ ).

According to what herein presented, in *Rusteel* project the effects of corrosion phenomena on the mechanical behaviour of steel reinforcements were investigated, in order to evaluate their consequences on both the tensile and seismic (LCF) behaviour. In particular, the experimental test campaign organized aims to the investigation of the effects of both chlorides and carbonation, and takes into account also the possible development of Hydrogen as a consequence of corrosion phenomena; Hydrogen content can lead to sudden brittle failures of rebars.

Two different protocols, one for the execution of salt spray chamber tests, selected as the most convenient procedure in relation to the ratio between required exposure time and following effects on the specimens, and the other for immersion carbonation tests, selected for reproducing more uniform corrosion phenomena, were elaborated in collaboration with the other partners of the research project.

The protocol for salt spray chamber tests (based on ISO 9227 provisions) foresees the execution of wet/dry cycles of 90 minutes (90 minutes dry, 90 minutes wet, resulting in 8 cycles/day) with a pH of the salt spray chamber ranging between 5.5 and 6.2. Specimens of 500-600 mm length shall be opportunely protected with a wax cover leaving free to corrode only a central part of about 20 mm (i.e. the distance between two subsequently ribs); the specimens shall be positioned in salt spray chamber with a slope of 60° respect to the vertical walls of the chamber in order to prevent salt generation. After the end of the exposure period and before the execution of mechanical tests, steel corroded rebars shall be maintained at a temperature lower than -5°, in order to kept inside the Hydrogen volatile part eventually developed during corrosion process. The protocol for carbonation corrosion tests follows, for the preparation of the specimens, a procedure similar to the one used for salt spray chamber tests; the samples shall be immersed two different chemical solutions able to reproduce the effects of carbonation on rebars. A versatile and convenient apparatus, consisting of a box of suitable size (20-40 ml/cm<sup>2</sup> of exposed surface - at least 1.2 l for test specimen), shall be used. A temperature regulating device, a specimen support system and a suitable stirring mechanism are also needed. Two different solutions were selected, the first to simulate the pore liquid of alkaline and carbonated concrete and the second to reproduce heavier condition (at a lower pH, where no protective layer is formed). The composition of the test solutions are:

1. CaCO<sub>3</sub> (sat.) + SiO<sub>2</sub> (sat.) (pH=8.3)
2. CaCO<sub>3</sub> (sat.) + SiO<sub>2</sub> (sat.) + NaHCO<sub>3</sub> (25mM) + CaSO<sub>4</sub> (sat.) (pH=7.8)

Reduced sets of rebars, respect to the one presented in Table 2.1, were selected for the execution of carbonation corrosion tests on specimens: in Table 2.2 the chosen bars are listed.

Both monotonic and LCF tests shall be executed; nowadays, cyclic tests and carbonation corrosion process are ongoing, while some preliminary results of monotonic tensile tests from salt spray

chamber corrosion tests can be presented; in Figure 2.2, dashed lines represent the results of tensile tests on uncorroded rebars (reference bars). As visible, corrosion phenomena lead to some modifications both in strenght and in ductility: the reduction of the yielding strenght is evident especially after 90 days of exposure (Figure 2.2.a); the shape of the stress-strain diagram at yielding is also modified. Table 2.3 summarizes preliminary results obtained from tensile tests on different corroded bars; both modifications of strenght and ductility and mass loss are shown.

**Table 2.2.** Steel bars selected for salt-spray chamber tests and tests foreseen.

ID	Quality	$\phi$	Producer	Surface	Process	Salt Spray Tests (45 and 90 days)	Carbonation corrosion tests
1	B500B	16	2	Ribbed	TEMP	x	x
2	B450C	16	2	Ribbed	TEMP	x	x
3	B400C	16	2	Ribbed	TEMP	x	-
4	B400C	16	1	Ribbed	MA	x	-
5	B500A	12	1	Ribbed	CW	x	x
6	B500B	25	1	Ribbed	TEMP	x	-
7	B500B	12	2	Ribbed	STR	x	-
8	B400C	25	1	Ribbed	MA	x	-
9	B450C	12	2	Ribbed	STR	x	-
10	B450C	25	1	Ribbed	TEMP	x	-

**Table 2.3.** Results obtained from tensile tests on corroded steel bars (45 and 90 days).

BAR LABEL	REFERENCE			CORROSION 45 days				CORROSION 90 days			
	R <sub>e</sub>	R <sub>m</sub>	A <sub>gt</sub>	Mass Loss	R <sub>e</sub>	R <sub>m</sub>	A <sub>gt</sub>	Mass Loss	R <sub>e</sub>	R <sub>m</sub>	A <sub>gt</sub>
	MPa	MPa	%	%	MPa	MPa	%	%	MPa	MPa	%
B400C-16-TEMP-01	429	546	16.4	9.87	445	550	8.4	13.5	398	525	7.1
B400C-16-TEMP-02	438	542	15.6	13.9	449	548	7.5	18.9	401	521	5.8
B400C-16-TEMP-03	438	555	15.6	15.5	437	555	9.0	12.2	405	525	6.4
B400C-16-TEMP-04	-	-	-	-	-	-	-	15.9	417	519	7.5
B400C-16-TEMP-05	-	-	-	-	-	-	-	16.0	411	-	7.6
B450C-16-TEMP-01	508	611	13.8	7.9	509	614	6.9	14.6	481	600	4.3
B450C-16-TEMP-02	502	601	15.0	7.5	511	616	6.2	6.1	484	598	4.4
B450C-16-TEMP-03	510	687	12.0	11.1	504	608	5.7	8.7	500	611	5.1
B450C-16-TEMP-04	-	-	-	-	-	-	-	6.9	497	608	5.7
B450C-16-TEMP-05	-	-	-	-	-	-	-	8.3	481	600	4.1
B500B-16-TEMP-01	472	577	11.5	20.8	500	610	9.1	24.3	492	608	5.7
B500B-16-TEMP-02	503	687	13.9	19.1	491	604	6.3	17.0	476	596	4.6
B500B-16-TEMP-03	503	604	11.4	25.6	492	604	7.5	44.9	482	611	5.0
B500B-16-TEMP-04	-	-	-	-	-	-	-	16.9	485	606	5.1
B500B-16-TEMP-05	-	-	-	-	-	-	-	27.8	491	603	5.0
B500A-12-CW-01	568	572	7.5	17.2	490	512	1.3	-	-	-	-
B500A-12-CW-02	570	579	6.6	14.3	495	519	0.9	-	-	-	-
B500A-12-CW-03	553	565	6.4	22.5	499	518	0.8	-	-	-	-
B500B-25-TEMP-01	531	660	12.9	1.7	518	637	8.5	-	-	-	-
B500B-25-TEMP-02	526	687	13.1	1.9	524	643	9.3	-	-	-	-
B500B-25-TEMP-03	532	662	12.7	12.7	514	634	8.2	-	-	-	-
B450C-25-TEMP-01	505	634	14.4	0.4	500	622	9.1	-	-	-	-
B450C-25-TEMP-02	508	640	15.5	0.7	495	618	8.3	-	-	-	-
B450C-25-TEMP-03	502	630	15.1	0.8	497	617	8.5	-	-	-	-
B400C-25-MA-01	433	577	20.0	0.7	428	576	11.6	-	-	-	-
B400C-25-MA-02	433	574	18.5	0.9	426	576	2.7	-	-	-	-
B400C-25-MA-03	420	565	16.7	0.7	424	576	13.3	-	-	-	-

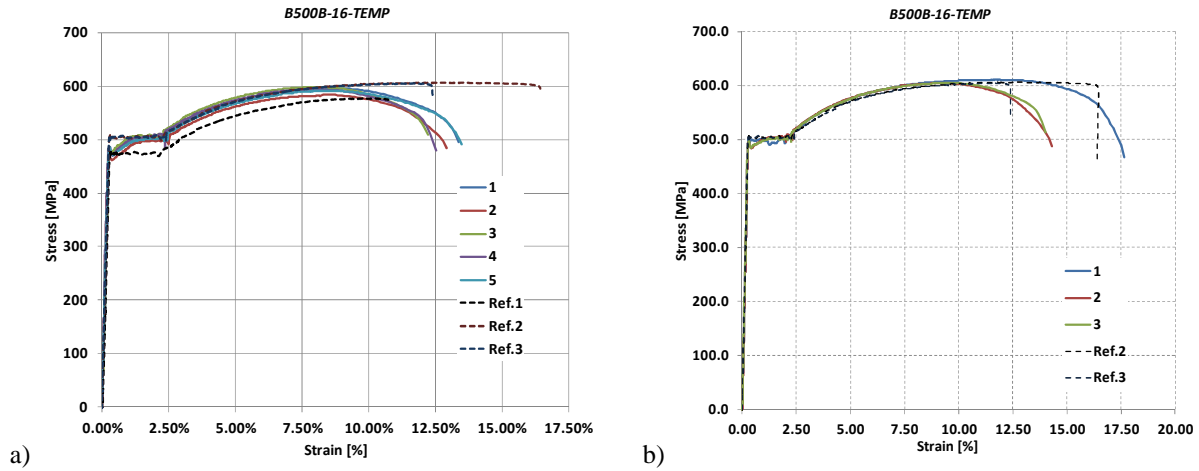


**Figure 2.2.** Stress-Strain diagrams for B500B-16-Tempcore after a) 90 days of exposure, b) 45 days of exposure.

## 4. DUCTILITY DEMAND OF STEEL REINFORCEMENTS

### 4.1. Design of buildings and elaboration of non linear models

Different r.c. buildings were designed according to the actual design standards prescriptions (Eurocode 8 and D.M. 14/01/2008); different functional destinations and plan schemes were selected. Buildings were designed considering different levels of p.g.a. (0.25g and 0.15g for high or medium seismicity area), different levels of ductility (HDC or LDC) and different steel grades for reinforcements (B450C, B400C and B500B), in order to represent the effective European scenario of constructions. In the present paper, preliminary results related to a residential building in HDC are presented.

Non linear fibre models were elaborated using OpenSees software for the execution of IDA analyses. Beams and columns were modelled as “beam with hinge” elements, i.e. each structural element is divided into three parts, two plastic hinges of length  $L_p$  in correspondence of the ends, with opportune non linear constitutive laws for concrete and steel, and an elastic central part; this kind of modelling allows the achievement of reduced computational times respect to the use of “non linear beam-column element” (Mazzoni et al. 2007). For the constitutive law of concrete the Braga-Gigliotti-Laterza (BGL) model, recently implemented in OpenSees (D’Amato 2008), was used; this model is able to directly take into account the confinement effects due to both longitudinal and transversal reinforcements layout. For the constitutive law of steel reinforcements, a new model, including slip phenomena between the rebar and the surrounding concrete was elaborated: for increasing external actions, in fact, the relative displacement between concrete and rebars shall be taken into account since the differences between strains in bars and concrete can be significant.

In the present work, the tensile stress-slip ( $\sigma$ - $u$ ) model previously elaborated by D’Amato, Braga et al. (D’Amato 2008, Braga et al. 2009) was extended to the case of ribbed bars in new constructions, including some aspects (i.e. the real hardening behaviour of steel) not previously considered. The main assumptions at the base of the presented model are: 1) the relation between bond stress and slip ( $\tau$ - $u$ ) is elasto-plastic; 2) the tensile stress-strain ( $\sigma$ - $\epsilon$ ) law is elasto-plastic with hardening, and the slope of the hardening branch is defined with effective experimental tests executed on rebars; 3) the slip field is bi-linear, with a first branch characterizing the behaviour before yielding and a second branch, with slope increment, defining the behaviour in the hardening field; 4) the hooked end, if present, is represented by a linear elastic function according to what proposed in literature.

The stress-slip relation for ribbed rebars is obtained through the use of equilibrium, compatibility and constitutive laws equations. The relative simplified slip field along the bar can be expressed as presented in Eqn. 4.1, in which  $x$  is the general position along the length of the bar,  $L_y$  is the part of the rebar where the axial stress is higher than yielding stress ( $f_y$ ),  $L_0$  is the total anchorage length,  $u_y$  the value of the slip in correspondence of the free length when yielding is reached and  $u_L$  the free end slip in correspondence of the generic step of load. The axial stress on steel reinforcing rebars can be expressed as presented in Eqn. 4.2, in which the trend of bond stress is defined in relation to the value

of slip in the generic point of the rebar. The length of the part of the rebar in which the yielding strength is exceeded ( $L_y$ ) can be evaluated considering the equilibrium of forces at the two ends of the bar interested by slips (Eqn. 4.3). Using the following presented equations, the axial stress-slip relationship is evaluated. For the shift from a stress-slip ( $\sigma$ - $u$ ) to a stress-strain ( $\sigma$ - $\epsilon$ ) relationship, a simplifying operation using as parameter the length of plastic hinge  $L_p$  was used. For the definition of the plastic hinge length  $L_p$  of BWH elements, the formulation given by Panagiotakos and Fardis (2001) was used, putting the parameter  $a_{sl}$  equal to zero, since slippage phenomena were already taken into account in the constitutive model of material.

$$u(x) = \begin{cases} \frac{x}{L_0} \cdot u_L & \text{pre - yielding} \\ \frac{u_y}{L_0 - L_y} \cdot x & \text{post - yielding} \\ u_y + \frac{u_L - u_y}{L_y} \cdot (x - L_0 + L_y) & \text{if } L_0 - L_y < x \leq L_0 \end{cases} \quad (4.1)$$

$$\sigma(x) = \frac{1}{A_b} \int \tau(x) \cdot \pi \phi \, dx \quad (4.2)$$

$$\int_0^{L_0 - L_y} \pi D \tau(x) dx = \frac{\pi D^2}{4} f_y \quad (4.3)$$

## 4.2. Procedure for the selection of earthquakes for Incremental Dynamic Analyses

A preliminary selection of the most significant time histories included in the European Strong Motion Database was executed, in order to individuate homogeneous classes of earthquakes characterized by specific soil conditions and magnitude ranges. All the accelerograms were analyzed in order to evaluate their number of cycles ( $N_{cycles}$ ) and their maximum amplitude ( $\Delta_{p.g.a.}$ ), grouping them into four different classes of amplitude in relation to the level of peak ground acceleration (p.g.a.): lower than 0.25 p.g.a., between 0.25 and 0.50 p.g.a., between 0.50 and 0.75 p.g.a. and higher than 0.75 p.g.a.

The increase of  $\Delta_{p.g.a.}$  (or of p.g.a.) leads to the decrease of  $N_{cycles}$ : for strong earthquakes the seismic demand involves only few cycles, characterized by a high variation of accelerations.

A first selection of time histories was executed considering only those earthquakes characterized by the maximization of  $N_{cycles}$  and/or  $\Delta_{p.g.a.}$ ; the final selection of the time histories for the numerical simulations, on the other hand, cannot neglect the dynamic characteristics of the building: the selected earthquakes shall be consequently re-analyzed considering the structural response of the case studies.

For each designed building, an opportune equivalent single degree of freedom (SDOF) characterized by specific hysteretic laws (Wayne Stewart –WS, Muto, and elastic perfectly plastic –EPP) shall be individuated and then analyzed to find the time histories able to maximize the damage level, expressed in terms of damage indicators (Park and Ang 1985, Krawinkler et al. 1994):

$$DI_{P\&A} = \frac{\delta_m}{\delta_u} + \frac{\beta \cdot E_h}{\delta_u \cdot P_y} \quad (a) \quad DI = N_{cycles} \Big|_{\mu_{req} \geq 2.0} \cdot \frac{\Delta_{max,cycle}}{2} \quad (b) \quad (4.4)$$

In which  $\delta_m$  and  $\delta_u$  are the maximum deformation and the collapse deformation of the SDOF system,  $E_h$  the hysteretic energy dissipated,  $P_y$  is the force corresponding to yielding;  $\beta$  is equal to 0.1.

$\mu_{req}$  is the required ductility of SDOF system subjected to the considered earthquake,  $\Delta_{max,cycle}$  is the maximum deformation (drift).

The analysis of the results obtained from SDOF systems under the pre-selected time histories, in terms of damage indicators (Figure 4.1), allows the individuation of the most dangerous seismic inputs to be



used in the numerical simulations for each structure, whose dynamic response is representative of the structural behaviour of the designed case study in terms of stiffness, yielding, shape of hysteresis.

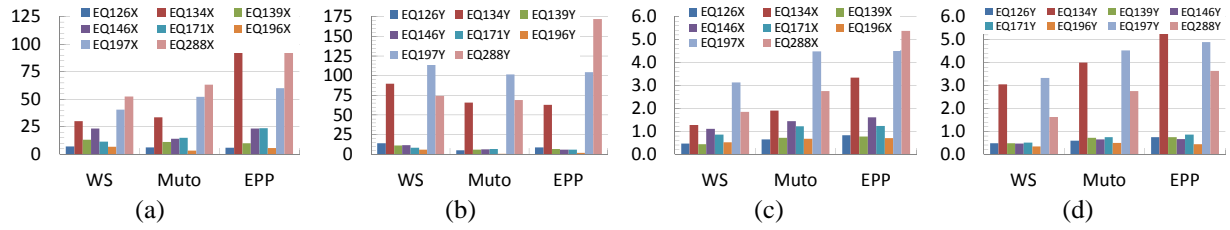


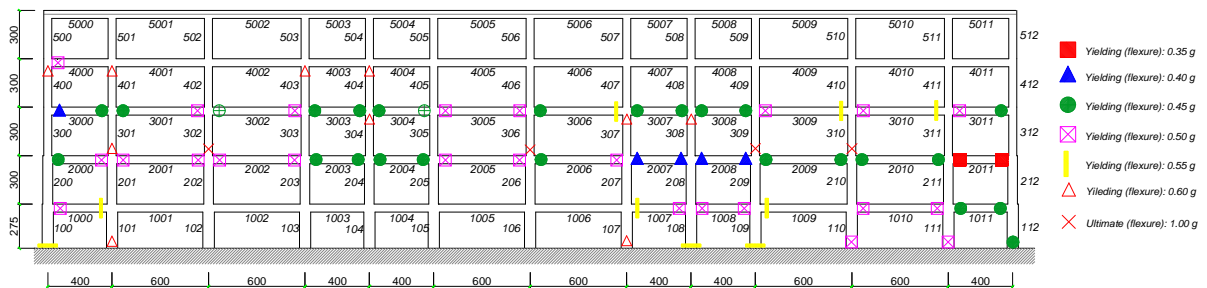
**Figure 4. 1.** Damage indicator obtained from executed simulations: a), b) time histories X and Y direction and DI (eqn. 4.4b); c), d) time histories X and Y direction and DI (eqn. 4.4a)

### 4.3. Execution of non linear analyses

Preliminary IDA analyses were executed using artificial accelerograms compatible with the soil characteristics and the design spectrum; the selection of the representative earthquakes to use is still ongoing. The mean real mechanical characteristics of steel reinforcements, coming from the experimental tensile tests executed on 9 different specimens of steel grade B450C (TempCore), diameter 16 mm were used: yielding strenght equal to 510 MPa, tensile strenght 610 MPa and  $A_{gt}$  equal to 12.4%. IDA were executed considering steps of p.g.a of 0.05g, until a maximum of 1.00 g; the design p.g.a. considered for the presented building was equal to 0.25g.

The seismic capacity of r.c. is evaluated following the prescriptions provided by Eurocode 8; in particular, for ductile elements, the two rotations corresponding to the yielding and to the ultimate conditions shall be evaluated, while for brittle elements both static and cyclic shear resistance are needed. Annex A of Eurocode 8 (UNI EN 1998-3:2005) provides the formula for the evaluation of chord rotation at yielding  $\theta_y$  and total chord rotation capacity  $\theta_{um}$  (respectively expressions A.10b and A.1), relative to the assessment at Damage Limitation limit state (DL) or at Near Collapse limit state (NC). Annex A also provides the expression for the evaluation of cyclic shear resistance (A.12) while the static one follows the formulation given by Eurocode 2 (UNI EN 1992-1-1:2005).

The evaluation of the structural behaviour of the selected building according to the expressions above listed, is summarized in the Figure 4.2: with the filled square the sections reaching their yielding capacity for p.g.a. equal to 0.35 g are evidenced, with the filled triangle the ones reaching  $\theta_y$  for p.g.a. equal to 0.40 g, the filled circle and the empty square represent those elements that reach the yielding respectively at 0.45 and 0.50 g and, finally the cross indicates the sections in which ultimate chord rotation occurs. For a p.g.a. level of 0.50 g a lot of structural elements are yielded (beams and columns of the first floor) but only for a very high level of p.g.a. (1.00 g) some elements reach the ultimate chord rotation limit (base section of 3<sup>rd</sup> floor columns and upper section of columns of the 4<sup>th</sup> floor). No shear mechanisms activate in beams or columns, underlining the quality of the design.



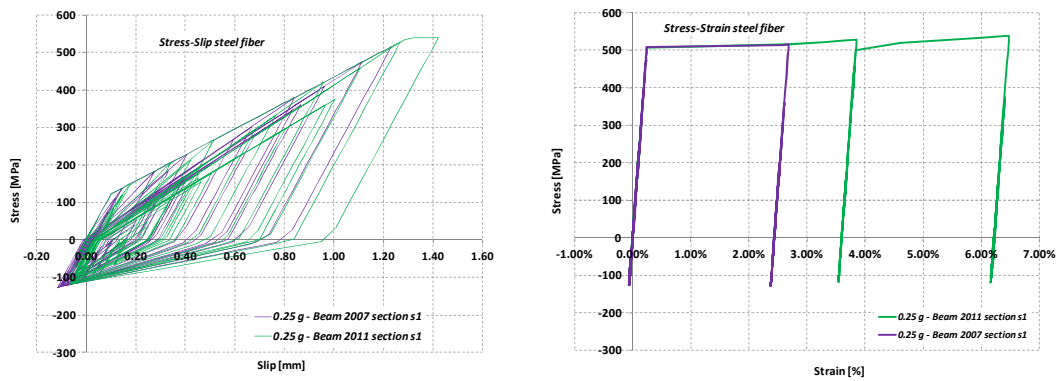
**Figure 4. 2.** Activation of ductile mechanisms in beams and columns.

Figure 4.2 allows the individuation of the structural elements reaching the yielding for lower levels of p.g.a., according to the conventional expressions provided by Eurocode 8 for the determination of  $\theta_y$ .



Moreover, the elaboration of non linear fibre models allows the individuation of the effective behaviour of steel reinforcing bars under seismic action, leading to the evaluation of the real maximum level of elongation imposed by the earthquake and, consequently, to the estimation of the ductility demand. Figure 4.3 shows some preliminary results of stress-strain diagrams on steel reinforcement fibres in beams 2007 and 2011 (between columns 107 - 108 and 111 - 112, Figure 4.2), for p.g.a. levels of 0.25 g (equal to the one used in the desing), while Figure 4.4 presents the behaviour of steel fibres in column n°107 and n°108 for a p.g.a. level equal to 0.45 g. The maximum level of strain reached in steel reinforcing bars in the selected beams is equal to 2,68% and 6,47% respectively, while in the columns, the required ductility is equal to 4.98% for column 107 and 6.42% for column 108, for p.g.a. equal to 0.45 g (at 0.25 g rebars are still in the elastic field).

It's necessary to underline that the results herein presented are obtained from non linear analyses executed using artificial accelerograms: further investigations, using real natural time histories, opportunely selected according to what presented at paragraph 4.2 are already ongoing.



**Figure 4. 3.** a) Stress-slip and b) stress-strain diagrams for bar B450C (16mm), beams 2007 and 2011, 0.25 g.

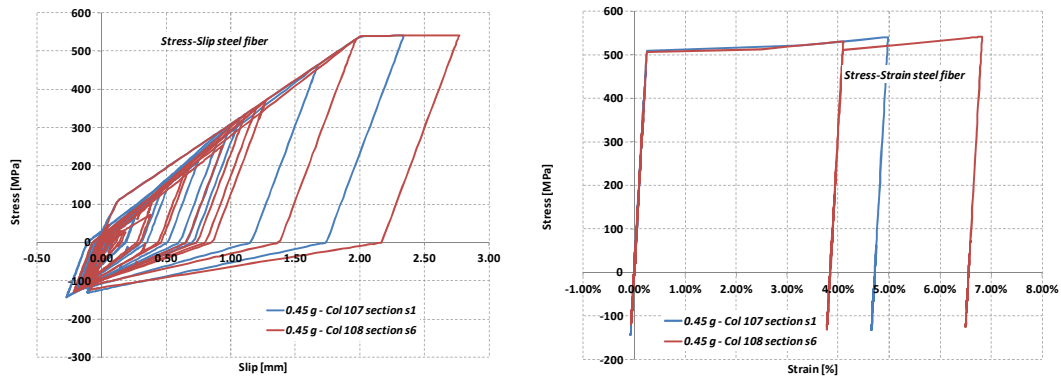


**Figure 4. 4.** a) Stress-slip and b) stress-strain diagrams for bar B450C (16mm), columns 107 and 108, 0.45 g.

## 5. CONCLUSIONS AND FUTURE DEVELOPMENTS

The preliminary results of *Rusteel* research project, both for what related to the ductility capacity and ductility demand, are presented. The seismic mechanical behaviour of steel reinforcements of uncorroded and corroded rebars (*capacity*) was evaluated through the execution of experimental tensile and low-cycle fatigue tests, following specific protocols opportunely elaborated inside the research project and described in the present paper.

The execution of experimental tests on corroded steel reinforcing bars showed the influence of corrosion phenomena on the reduction of mechanical properties, both in terms of strenght and ductility ( $A_{gt}$ ), evidencing the necessity of accurate numerical analyses aiming to the understanding the effective ductility *demand* imposed by earthquakes to r.c. buildings. In particular, in the present paper, the methodology adopted for the evaluation of the level of ductility required by seismic action to an

ordinary r.c. residential building is showed, including the description of the procedure for the opportune selection of time histories for IDA analyses.

A new constitutive law for steel reinforcements, able to take into account the effects of slip between bars and surrounding concrete, was elaborated on the base of the model proposed by D'Amato, Braga et al. (2008) and then modified to consider strain-hardening phenomena. Preliminary Incremental Dynamic Analyses executed using artificial accelerograms are presented, evidencing the level of strain imposed to rebars in r.c. buildings. Further investigations and simulations about both ductility *demand* and *capacity* evaluation are still ongoing.

## REFERENCES

- Apostolopoulos, C. A., Michalopoulos, D. (2006). Effect of Corrosion on Mass Loss, and High and Low Cycle Fatigue of Reinforcing Steel. *Journal of Materials Engineering and Performance* **15:6**, 742-749.
- Apostolopoulos, C.A. (2007). Mechanical behavior of corroded reinforcing steel bars S500s Tempcore under low cycle fatigue. *Construction and Building Materials* **21**, 1447-1456.
- Apostolopoulos, C.A., Papadakis, V.G. (2008). Consequences of steel corrosion on the ductility properties of reinforcement bar. *Construction and Building Materials* **22**, 2316-2324.
- Apostolopoulos, C.A., Papadopoulos, M.P. (2007). Tensile and low cycle fatigue behavior of corroded reinforcing steel bars S400. *Construction and Building Materials* **21**, 855-864.
- Braga, F., D'Amato, M., Gigliotti, R., Laterza, M. (2009). Analisi non lineari di strutture in c.a.: implementazione in OpenSees del modello BGL di calcestruzzo confinato. *XIII Congresso Nazionale ANIDIS, l'ingegneria Sismica in Italia*.
- Crespi, P. (2002). Monotonic and cyclic behaviour of rebars in the plastic hinge of r.c. beams. PhD Thesis, University of Milano.
- D. M. Infrastrutture Trasporti 14 gennaio 2008, Norme Tecniche per le Costruzioni NTC 2008.
- D'Amato, M. (2008). Analytical models for non linear analysis of RC structures: confined concrete and bond-slips of longitudinal bars. PhD Thesis, University of Basilicata.
- European Commission (EC), M/115 rev.1 EN, Revised mandate M115 to CEN/CENELEC concerning the execution of standardisation work for harmonized standards on Reinforcing and prestressing (for concrete), Brussels May 26th 2009.
- Hawileh, R. A., Abdalla, J. A., Oudah, F., Abdelrahman, K. (2010). Low-cycle fatigue life behaviour of BS 460B and BS B500B steel reinforcing bars. *Fatigue & Fracture of Engineering Materials & Structures* **33:7**, 397-407.
- Krawinkler, H., Parisi, F., Ibarra, L., Ayoub, A., Medina, R. (1994). W02-Development of a testing protocol for Woodframe Structures. *CalTech Woodframe project - CUREE Publications*.
- LNEC E455-2008 – Varoes de aço A400 NR de ductilidade especial para armaduras de betão armado: características, ensaios e marcação.
- LNEC E460-2008 – Varoes de aço A500 NR de ductilidade especial para armaduras de betão armado: características, ensaios e marcação.
- Mander, J.B., Panthaki, F.D., Kasalanati, A. (1994). Low-cycle fatigue behaviour of reinforcing steel. *Journal of Materials in Civil Engineering* **6:4**, 453-467.
- Mazzoni, S., McKenna, F., Scott, M. H. et al. (2007). *OpenSees command Language Manual*.
- Panagiotakos, T.B., Fardis, M.N. (2001). Deformations of Reinforced Concrete Members at Yielding and Ultimate. *ACI Structural Journal* **98:2**, 135-148.
- Park, Y.J., Ang, A.H-S. (1985). Seismic damage analysis of RC buildings. *Journal of Structural Engineering* **ST4:111**, 740-757.
- Rodriguez, M.E., Botero, J.C., Villa, J. (1999). Cyclic stress-strain behaviour of reinforcing steel including effect of buckling. *Journal of Structural Engineering* **125:6**, 605-612.
- UNE 36065 EX, Norma Española Experimental 2000 – Barras corrugadas de acero soldable con características especiales de ductilidad para armaduras de horigòn armado, 2000.
- UNI EN 1992-1-1:2005, Eurocode 2 - Design of concrete structures - Part 1-1: General rules and rules for buildings, 2005.
- UNI EN 1992-1-1:2005, Eurocode 2 (Annex C) - Design of concrete structures - Part 1-1: General rules and rules for buildings, 2005
- UNI EN 1998-1:2005, Eurocode 8 - Design of structures for earthquake resistance - Part 1: General rules, seismic actions and rules for buildings, 2005
- UNI EN ISO 9227:2006 Corrosion tests in artificial atmospheres - Salt spray tests.